International Journal of Informatics and Communication Technology (IJ-ICT)
Vol. 14, No. 3, December 2025, pp. 1172~1178
ISSN: 2252-8776, DOI: 10.11591/ijict.v14i3.pp1172-1178

Pneumonia detection system using convolutional neural network with DenseNet201 architecture

Muhammad Qomaruddin, Andi Riansyah, Hildan Mulyo Hermawan, Moch Taufik
Department of Informatics Enginering, Faculty of Industrial Technology, Universitas Islam Sultan Agung, Semarang, Indonesia

Article Info

Article history:

Received Sep 18, 2024
Revised Mar 25, 2025
Accepted Jul 1, 2025

Keywords:

Classification
DenseNet201
Optimizer
Pneumonia
X-ray

ABSTRACT

The diagnosis of pneumonia remains a significant challenge for medical practitioners worldwide, particularly in regions with limited healthcare resources. Traditional interpretation of chest X-rays is time-consuming and often subjective, especially when images are of low quality. This study presents the development of a web-based system utilizing the DenseNet201 architecture to address these challenges. A series of experiments were conducted to evaluate three optimizers Adam, Adamax, and Adadelta over fifty epochs. Among them, Adamax yielded the best performance, achieving a training accuracy of 93.67% and a validation accuracy of 94.20%. When tested on new data, the system consistently delivered high performance, with accuracy, precision, recall, and F1 score all reaching 96%. These results suggest that the proposed system has the potential to significantly enhance the accuracy and efficiency of pneumonia diagnosis based on chest X-rays.

Corresponding Author:

Muhammad Qomaruddin
Department of Informatics Engineering, Faculty of Industrial Technology
Sultan Agung Islamic University
Jl. Raya Kaligawe Km. 4, Semarang 50112, Indonesia
Email: mqomaruddin@unissula.ac.id

1. INTRODUCTION

Pneumonia, a sudden and severe inflammation of the lungs, remains a major global health issue [1]. This respiratory condition can be caused by various pathogens, including bacteria such as *Streptococcus pneumoniae* and *Haemophilus influenzae*, viruses like influenza and respiratory syncytial virus (RSV), fungi such as *Pneumocystis jirovecii*, and even parasites. Clinically, pneumonia manifests with a range of symptoms, including cough (which may produce sputum), fever, chills, difficulty breathing, chest pain (particularly with deep breathing or coughing), rapid breathing, fatigue, and in some cases, nausea, vomiting, or confusion [2], [3].

Vulnerable populations, especially children and the elderly, bear a disproportionate burden of pneumonia. In 2019, over 740,000 children under the age of five died from pneumonia worldwide, with the highest mortality rates observed in regions with limited access to healthcare, such as South Asia and sub-Saharan Africa [4]. However, pneumonia remains a global concern, affecting individuals worldwide, particularly those with compromised immune systems, chronic conditions, or exposure to environmental hazards like air pollution and cigarette smoke. While pneumonia can be life-threatening, it is not invincible. Preventive measures such as immunization against common respiratory pathogens, basic hygiene practices, and management of underlying health conditions can significantly reduce the risk of developing pneumonia. Early diagnosis and appropriate treatment with antibiotics, antivirals, or antifungals, depending on the causative agent can lead to favorable outcomes for most patients [5], [6].

Artificial intelligence (AI), particularly convolutional neural networks (CNNs), has emerged as a transformative tool in medical imaging and diagnostics [7]-[9]. CNNs, inspired by the human visual system, are adept at identifying patterns in images, making them highly effective for analyzing medical scans such as chest X-rays. Through training on large, labeled datasets, CNNs can learn to differentiate pneumonia from other lung conditions or normal lung tissue, recognizing subtle visual cues that may be missed by the human eye. This technology holds the potential to revolutionize pneumonia diagnosis by enabling faster, more accurate, and widely accessible screening, particularly in resource-limited settings [7], [9]-[11].

This study aims to leverage AI to develop an advanced diagnostic tool using DenseNet201, a state-of-the-art CNN architecture known for its exceptional accuracy in image classification tasks [12], [13]. The goal is to create a web-based platform that allows healthcare professionals to upload chest X-ray images for analysis. The system will utilize the trained DenseNet201 model to assess the likelihood of pneumonia, providing clinicians with valuable insights to support diagnostic decision-making and treatment planning [14], [15]. This AI-driven solution has the potential to alleviate the burden on radiologists, reduce diagnostic errors, and improve patient outcomes by automating and expediting the image analysis process. However, the integration of AI in healthcare presents its own set of challenges [16]-[18]. To ensure the ethical and equitable deployment of AI-based diagnostic tools, it is essential to address concerns related to data privacy, algorithmic bias, and the potential for over-reliance on automated systems [19], [20].

2. METHOD

2.1. Dataset preparation and preprocessing

Our study utilized a comprehensive lung image dataset, consisting of 1,583 normal cases and 4,273 pneumonia cases, creating a total of 5,856 chest X-ray images. The dataset's diversity, which included a wide range of pneumonia types and normal lung morphologies, was crucial for the development and validation of a robust diagnostic model. To ensure reproducibility, the dataset was systematically organized and validated before processing [2], [21]. The dataset is split using the holdout validation technique, with a ratio of 80:20 for training and validation sets [22]-[24]. This resulted in 4,685 images for training (3,178 pneumonia cases and 1,507 normal cases) and 1,171 images for validation (1,095 pneumonia cases and 76 normal cases), as detailed in Table 1.

Table 1. Split dataset into training and validation

Data	Percentage	Pneumonia	Normal	Total data
Training	80%	4204	1026	3178
Validation	20%	1052	257	795

2.2. Image preprocessing and augmentation

Before model training, all images underwent standardized preprocessing procedures. The dataset was normalized using an input preprocess function implemented through the preprocessing option in the ImageDataGenerator class. This function ensures that pixel values are scaled to the range [0,1], fitting within the expected input range for the DenseNet architecture.

To improve model generalization and reduce overfitting issues, comprehensive image augmentation techniques were systematically applied during training:

- Image resizing to 224×224 pixels to match DenseNet201 input requirements
- Width and height shift range of 0.2
- Shear transformation with range of 0.2
- Rotation range of 20 degrees
- Zoom range of 0.2
- Horizontal flip enabled
- Fill mode set to 'nearest'

These augmentation parameters were empirically determined to introduce sufficient variability while maintaining image integrity [25]-[27].

2.3. Model architecture and configuration

The experimental framework employed a transfer learning approach using the pre-trained DenseNet201 model. The complete model architecture was configured as follows:

i) Base model configuration**:**
   - Input dimensions: 224×224 pixels, 3 color channels (RGB)
   - Base model: DenseNet201 (excluding the top fully connected layer)

- Initial weights: pre-trained on ImageNet dataset
- Trainability: all layers in the DenseNet201 base model were frozen (set to non-trainable) to preserve pre-trained features and optimize computational efficiency

ii) Custom classification head: the model architecture was enhanced with custom layers for binary classification:
- GlobalAveragePooling2D layer to reduce spatial dimensions
- Dense layer with 256 units and rectified linear unit (ReLU) activation function
- Dropout layer with rate = 0.4 for regularization and overfitting mitigation
- Final Dense layer with 1 unit and sigmoid activation function for binary output

This architecture generally consists of several blocks called "Dense Blocks", followed by down sampling layers such as pooling or convolution with steps to reduce the spatial dimension. The DenseNet201 architecture is shown in Figure 1.

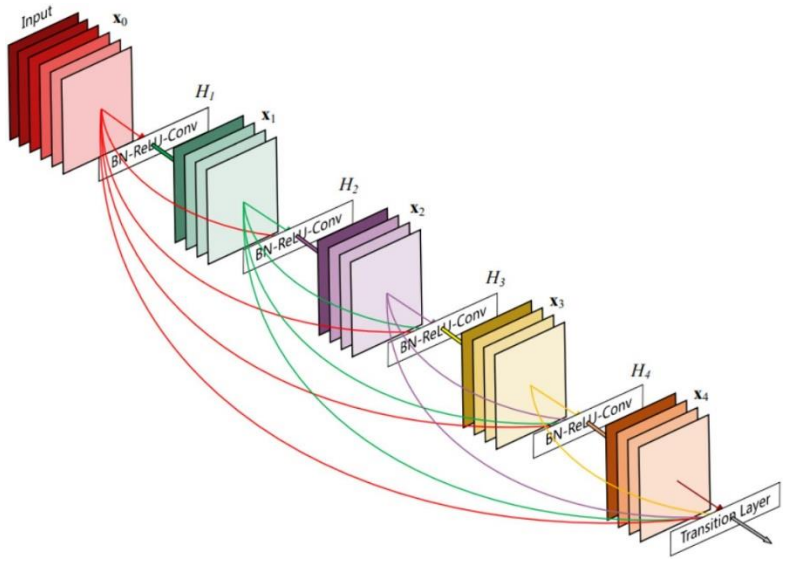

Figure 1. DenseNet201 architecture

2.4. Training configuration and optimization

To address the class imbalance in the dataset (pneumonia cases: 4,273 vs normal cases: 1,583), class weights were calculated using the formula: class_weight = n_samples/(n_classes×np.bincount(y)) and applied during model training [28], [29].

Three different optimization algorithms were systematically evaluated:
- Adam optimizer: adaptive learning rate with β_1=0.9, β_2=0.999
- Adamax optimizer: variant of Adam based on infinity norm with β_1=0.9, β_2=0.999
- Adadelta optimizer: adaptive learning rate method with ρ=0.95

Training parameters:
- Learning rate: 0.001 for all optimizers
- Batch size: 128
- Maximum epochs: 50
- Loss function: binary cross-entropy
- Evaluation metric: binary accuracy
- Early stopping: enabled with patience=10 and validation loss monitoring
- Model checkpoint: best weights saved based on validation accuracy

2.5. Experimental procedure

The experimental procedure was conducted in the following systematic steps:

i) Data loading: chest X-ray images loaded and organized into training/validation directories
ii) Data generators: ImageDataGenerator instances created with specified augmentation parameters
iii) Model compilation: DenseNet201 models compiled with different optimizers

iv) Training phase: models trained for up to 50 epochs with early stopping
v) Evaluation phase: best models evaluated on validation set
vi) Performance analysis: metrics calculated including accuracy, precision, recall, and F1-score

This methodology ensures reproducibility and allows for systematic comparison of optimizer performance on pneumonia detection tasks [25], [26], [30].

3. RESULTS AND DISCUSSION

Table 2 presents a comparison of three optimization algorithms Adam, Adamax, and Adadelta during the model training process. The table shows the number of epochs completed, as well as the loss and binary accuracy values for both training and validation data, along with the learning rate used. Adam completed 19 epochs out of the planned 50, achieving a training loss of 0.2358 and a binary accuracy of 0.9298. For the validation data, Adam achieved a validation loss of 0.2207 and a validation binary accuracy of 0.9316.

Table 2. Result of training data use DenseNet

Variable	Epoch	Loss	Binary accuracy	Val-loss	Val-binary accuracy	learning rate
Adam	19/50	0.2358	0.9298	0.2207	0.9316	0.001
Adamax	26/50	0.2881	0.9367	0.2603	0.9420	0.001
Adadelta	50/50	4.6946	0.8264	4.7140	0.8137	0.001

Adamax completed 26 epochs, achieving a training loss of 0.2881 and binary accuracy of 0.9367. For validation data, Adamax reached a validation loss of 0.2603 and validation binary accuracy of 0.9420. Adadelta was the only optimizer to complete all 50 epochs, but it exhibited significantly higher loss values compared to the other two algorithms, with a training loss of 4.6946 and validation loss of 4.7140. Adadelta's binary accuracy was also lower, with values of 0.8264 for training and 0.8137 for validation. All algorithms utilized the same learning rate of 0.001.

Figure 2 shows the results of an X-ray of the lungs infected with pneumonia. With a red display and a score of 96%. A comparative analysis of the Adam, Adamax, and Adadelta optimization algorithms revealed notable differences in their performance throughout the training process. These results highlight the significant impact of optimization choice on model performance. Both Adam and Adamax demonstrated strong efficacy, achieving lower loss values and higher binary accuracy on both the training and validation datasets, despite not completing the full 50-epoch training schedule. Among them, Adamax showed slightly superior performance, reaching the highest validation accuracy of 0.9420 and progressing through more epochs (26) than Adam (19).

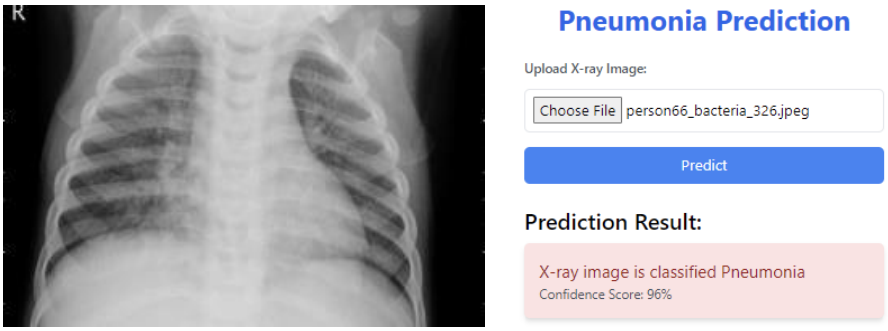

Figure 2. X-ray image detector using DenseNet201 architecture

4. CONCLUSION

This study highlights the effectiveness of the DenseNet201 architecture for pneumonia detection from chest X-rays, presenting several key findings. The Adamax optimizer was identified as the most effective, achieving the highest validation accuracy of 0.9420 and demonstrating superior performance metrics across all evaluations. Interestingly, the number of epochs completed was not a reliable predictor of model performance, as evidenced by Adadelta's subpar results despite completing all 50 epochs. The model demonstrated exceptional performance on independent test data, with accuracy, precision, recall, and F1

scores all reaching 0.96, confirming its practical applicability in clinical settings. These results suggest significant potential for enhancing the efficiency and accuracy of pneumonia detection. Future research should focus on validating these results across diverse datasets and clinical environments, exploring the factors that influence optimizer performance, and developing strategies for integrating the model into clinical workflows. This study contributes to the advancement of automated medical image analysis, offering a promising solution to improve pneumonia diagnosis in clinical practice.

FUNDING INFORMATION

Authors state no funding involved.

AUTHOR CONTRIBUTIONS STATEMENT

Name of Author	C	M	So	Va	Fo	I	R	D	O	E	Vi	Su	P	Fu
Muhammad Qomaruddin	✓	✓	✓	✓	✓	✓		✓	✓	✓			✓	✓
Andi Riansyah	✓	✓	✓		✓	✓		✓	✓	✓	✓	✓		
Hildan Mulyo Hermawan	✓		✓	✓			✓			✓	✓		✓	
Moch Taufik		✓			✓				✓	✓			✓	✓

C : **C**onceptualization
M : **M**ethodology
So : **So**ftware
Va : **Va**lidation
Fo : **Fo**rmal analysis
I : **I**nvestigation
R : **R**esources
D : **D**ata Curation
O : Writing - **O**riginal Draft
E : Writing - Review & **E**diting
Vi : **Vi**sualization
Su : **Su**pervision
P : **P**roject administration
Fu : **Fu**nding acquisition

CONFLICT OF INTEREST STATEMENT

The authors declare that there are no known conflicts of interest, either financial or non-financial, related to this research. All stages of the research and writing of this article were conducted independently and without any external influence. This article is the result of collaboration between a team of academic researchers and students from Universitas Islam Sultan Agung.

DATA AVAILABILITY

The data that support the findings of this study are available from the corresponding author upon reasonable request. The data consist of anonymized chest X-ray images used for model training and validation, and cannot be made publicly available due to privacy restrictions and licensing agreements.

REFERENCES

[1] A. G. Mathioudakis *et al.*, "Clinical trials of pneumonia management assess heterogeneous outcomes and measurement instruments," *Journal of Clinical Epidemiology*, vol. 164, pp. 88–95, Dec. 2023, doi: 10.1016/j.jclinepi.2023.10.011.

[2] T. Miyazaki *et al.*, "Community-acquired pneumonia incidence in adults aged 18 years and older in Goto City, Japan," *CHEST Pulmonary*, vol. 1, no. 2, p. 100007, Sep. 2023, doi: 10.1016/j.chpulm.2023.100007.

[3] K. Nakashima *et al.*, "Effectiveness of the 23-valent pneumococcal polysaccharide vaccine against community-acquired pneumonia in older individuals after the introduction of childhood 13-valent pneumococcal conjugate vaccine: a multicenter hospital-based case-control study in Japan," *Vaccine*, vol. 40, no. 46, pp. 6589–6598, Nov. 2022, doi: 10.1016/j.vaccine.2022.09.055.

[4] S. Hooli *et al.*, "In-hospital mortality risk stratification in children aged under 5 years with pneumonia with or without pulse oximetry: a secondary analysis of the pneumonia research partnership to assess who recommendations (PREPARE) dataset," *International Journal of Infectious Diseases*, vol. 129, pp. 240–250, Apr. 2023, doi: 10.1016/j.ijid.2023.02.005.

[5] J. Johnstone *et al.*, "Definitions, rates and associated mortality of ICU-acquired pneumonia: a multicenter cohort study," *Journal of Critical Care*, vol. 75, p. 154284, Jun. 2023, doi: 10.1016/j.jcrc.2023.154284.

[6] O. Marcy *et al.*, "Effect of systematic tuberculosis detection on mortality in young children with severe pneumonia in countries with high incidence of tuberculosis: a stepped-wedge cluster-randomised trial," *The Lancet Infectious Diseases*, vol. 23, no. 3, pp. 341–351, Mar. 2023, doi: 10.1016/S1473-3099(22)00668-5.

[7] H. Bai, "Convolutional neural network and recommendation algorithm for the new model of college music education," *Entertainment Computing*, vol. 48, p. 100612, Jan. 2024, doi: 10.1016/j.entcom.2023.100612.

[8] D. Mavaluru *et al.*, "Deep convolutional neural network based real-time abnormal behavior detection in social networks," *Computers and Electrical Engineering*, vol. 111, p. 108987, Nov. 2023, doi: 10.1016/j.compeleceng.2023.108987.

[9] M. T. Khan, "A modified convolutional neural network with rectangular filters for frequency-hopping spread spectrum signals," *Applied Soft Computing*, vol. 150, p. 111036, Jan. 2024, doi: 10.1016/j.asoc.2023.111036.

[10] Z. Wang *et al.*, "Machining feature process route planning based on a graph convolutional neural network," *Advanced Engineering Informatics*, vol. 59, p. 102249, Jan. 2024, doi: 10.1016/j.aei.2023.102249.
[11] J. Chen, Z. Zhao, and J. Zhang, "Predicting peak shear strength of rock fractures using tree-based models and convolutional neural network," *Computers and Geotechnics*, vol. 166, p. 105965, Feb. 2024, doi: 10.1016/j.compgeo.2023.105965.
[12] A. Marwanto, A. Riansyah, and M. K. Anwar, "An improvement of apple leaf diseases detection using convolutional neural network methods based on mobile systems," in *2024 11th International Conference on Electrical Engineering, Computer Science and Informatics (EECSI)*, Sep. 2024, pp. 440–447. doi: 10.1109/EECSI63442.2024.10776345.
[13] A. Riansyah, M. Qomaruddin, M. Indriastuti, and M. Sagaf, "Clustering digital transformation of small and medium enterprises (SMEs) using Fuzzy K-means method," in *2023 10th International Conference on Electrical Engineering, Computer Science and Informatics (EECSI)*, Sep. 2023, pp. 540–544. doi: 10.1109/EECSI59885.2023.10295664.
[14] L. Yang, C. Fan, H. Lin, and Y. Qiu, "Rema-Net: an efficient multi-attention convolutional neural network for rapid skin lesion segmentation," *Computers in Biology and Medicine*, vol. 159, p. 106952, Jun. 2023, doi: 10.1016/j.compbiomed.2023.106952.
[15] X. Qin, M. Liu, and G. Liu, "ResCNNT-fold: combining residual convolutional neural network and transformer for protein fold recognition from language model embeddings," *Computers in Biology and Medicine*, vol. 166, p. 107571, Nov. 2023, doi: 10.1016/j.compbiomed.2023.107571.
[16] S. Tyagi, D. T. Kushnure, and S. N. Talbar, "An amalgamation of vision transformer with convolutional neural network for automatic lung tumor segmentation," *Computerized Medical Imaging and Graphics*, vol. 108, p. 102258, Sep. 2023, doi: 10.1016/j.compmedimag.2023.102258.
[17] W. Chen and M. Li, "Standardized motion detection and real time heart rate monitoring of aerobics training based on convolution neural network," *Preventive Medicine*, vol. 174, p. 107642, Sep. 2023, doi: 10.1016/j.ypmed.2023.107642.
[18] J. E. Lee, H.-J. Jeon, O.-J. Lee, and H. G. Lim, "Diagnosis of diabetes mellitus using high frequency ultrasound and convolutional neural network," *Ultrasonics*, vol. 136, p. 107167, Jan. 2024, doi: 10.1016/j.ultras.2023.107167.
[19] B. Jafrasteh, S. P. Lubián-López, and I. Benavente-Fernández, "A deep sift convolutional neural networks for total brain volume estimation from 3D ultrasound images," *Computer Methods and Programs in Biomedicine*, vol. 242, p. 107805, Dec. 2023, doi: 10.1016/j.cmpb.2023.107805.
[20] T. Fan *et al.*, "A new deep convolutional neural network incorporating attentional mechanisms for ECG emotion recognition," *Computers in Biology and Medicine*, vol. 159, p. 106938, Jun. 2023, doi: 10.1016/j.compbiomed.2023.106938.
[21] A. Saidi, S. Ben Othman, M. Dhouibi, and S. Ben Saoud, "CNN inference acceleration on limited resources FPGA platforms_epilepsy detection case study," *IJ-ICT*, vol. 12, no. 3, p. 251, Dec. 2023, doi: 10.11591/ijict.v12i3.pp251-260.
[22] Md. S. H. Talukder *et al.*, "JutePestDetect: an intelligent approach for jute pest identification using fine-tuned transfer learning," *Smart Agricultural Technology*, vol. 5, p. 100279, Oct. 2023, doi: 10.1016/j.atech.2023.100279.
[23] M. G. Lanjewar, K. G. Panchbhai, and P. Charanarur, "Lung cancer detection from CT scans using modified DenseNet with feature selection methods and ML classifiers," *Expert Systems with Applications*, vol. 224, p. 119961, Aug. 2023, doi: 10.1016/j.eswa.2023.119961.
[24] A. Dash, P. K. Sethy, and S. K. Behera, "Maize disease identification based on optimized support vector machine using deep feature of DenseNet201," *Journal of Agriculture and Food Research*, vol. 14, p. 100824, Dec. 2023, doi: 10.1016/j.jafr.2023.100824.
[25] D. A. Sant'Ana *et al.*, "Computer vision system for superpixel classification and segmentation of sheep," *Ecological Informatics*, vol. 68, p. 101551, May 2022, doi: 10.1016/j.ecoinf.2021.101551.
[26] A. Sharma and P. K. Mishra, "Covid-MANet: multi-task attention network for explainable diagnosis and severity assessment of COVID-19 from CXR images," *Pattern Recognition*, vol. 131, p. 108826, Nov. 2022, doi: 10.1016/j.patcog.2022.108826.
[27] N. T. Le *et al.*, "Deep learning approach for age-related macular degeneration detection using retinal images: efficacy evaluation of different deep learning models," *Egyptian Informatics Journal*, vol. 24, no. 4, p. 100402, Dec. 2023, doi: 10.1016/j.eij.2023.100402.
[28] C. Wang, M. Sun, L. Liu, W. Zhu, P. Liu, and X. Li, "A high-accuracy genotype classification approach using time series imagery," *Biosystems Engineering*, vol. 220, pp. 172–180, Aug. 2022, doi: 10.1016/j.biosystemseng.2022.06.002.
[29] B. Dey, J. Ferdous, R. Ahmed, and J. Hossain, "Assessing deep convolutional neural network models and their comparative performance for automated medicinal plant identification from leaf images," *Heliyon*, vol. 10, no. 1, p. e23655, Jan. 2024, doi: 10.1016/j.heliyon.2023.e23655.
[30] M. K. Bohmrah and H. Kaur, "Classification of Covid-19 patients using efficient fine-tuned deep learning DenseNet model," *Global Transitions Proceedings*, vol. 2, no. 2, pp. 476–483, Nov. 2021, doi: 10.1016/j.gltp.2021.08.003.

BIOGRAPHIES OF AUTHORS

Muhammad Qomaruddin obtained a Master's degree in information systems from the Institute of Science and Technology "AKPRIND" and thereafter pursued a master's and doctoral degree from the University of Technology of Malaysia. He possesses a wealth of knowledge and expertise in the field of information systems. Presently, he holds the position of deputy rector at Sultan Agung Islamic University. He can be contacted at email: mqomaruddin@unissula.ac.id.

Andi Riansyah is a computer scientist with a Bachelor of computer science degree from Sultan Agung Islamic University and a Master of information systems degree from Diponegoro University. Andi Riansyah possesses over 7 years of research experience and has acquired a profound understanding of computer science, making noteworthy contributions to scientific advancement. He can be contacted at email: andi@unissula.ac.id.

Hildan Mulyo Hermawan is a software engineer. His primary focus lies in computer science, particularly in the field of artificial intelligence, where he has completed numerous courses and research projects. Aside from his academic pursuits. He can be contacted at email: hildanmulyo@std.unissula.ac.id.

Moch Taufik is a computer scientist with a bachelor of computer science degree from Sultan Agung Islamic University and a master of information systems degree from Informatika Amikom Yogyakarta. He possesses over 7 years of research experience and has acquired a profound understanding of computer science, making noteworthy contributions to scientific advancement. He can be contacted at email: mtaufik@unissula.ac.id.